New Classes of Asymmetric Spatial-Temporal Covariance Models

Man Sik Park and Montserrat Fuentes[1]

Institute of Statistics Mimeo Series# 2584

SUMMARY

Environmental spatial data often show complex spatial-temporal dependency structures that are difficult to model and estimate due to the lack of symmetry and other standard assumptions of the covariance function. In this study, we introduce certain types of symmetry in spatial-temporal processes: axial symmetry in time, axial symmetry in space, and diagonal symmetry in space, and propose new classes of asymmetric spatial-temporal covariance models by using spectral representations. We also explain the relationship between symmetry and separability and introduce nonseparable covariance models. Finally, we apply our new classes of covariance models to estimate the spatial-temporal structure of fine Particulate Matter ($PM_{2.5}$) over the northeastern region of U.S.

Key Words: Asymmetry; Nonseparability; Spatial-temporal process; Matérn covariance; Spectral density function

[1]M. S. Park is a graduate student in the Statistics Department at North Carolina State University (NCSU), Raleigh, NC 27695-8203. Tel.: (919) 515-7748, Fax: (919) 515-1169, E-mail: mspark@unity.ncsu.edu. M. Fuentes is an Associate professor in the Statistics Department, NCSU, Raleigh, NC 27695-8203, E-mail: fuentes@stat.ncsu.edu. This research was sponsored by a National Science Foundation grant DMS 0353029, and by a US EPA cooperative agreement.

Key words: Air pollution; Asymmetry; nonseparability; Spatial-temporal process; Matérn covariance; Spectral density function.

1 INTRODUCTION

Many studies in diverse fields such as climatology, ecology, and public health research show that environmental data have complex spatial-temporal dependency structures that are difficult to model and estimate. The spatial and the temporal structures are generally tied with each other in the spatial-temporal covariance functions, and it is not easy to model two structures simultaneously. In order to overcome the difficulty in modeling spatial-temporal processes, we usually assume separability and symmetry.

Separability in spatial-temporal processes enables us to easily construct the model due to advantages such as the simplified representation of the covariance matrix, and consequently, remarkable computational benefit. Suppose that $\{Z(\mathbf{s},t):\ \mathbf{s}\equiv(s_1,s_2,\cdots,s_d)'\in\mathbb{D}\subset\mathbb{R}^d,\ t\in[0,\infty)\}$ denotes a spatial-temporal process where $\mathbf{s}$ is a spatial location over a fixed domain $\mathbb{D}$, $\mathbb{R}^d$ is a d-dimensional Euclidean space, and t indicates time. Then the covariance function is defined as

$$C(\mathbf{s}_i-\mathbf{s}_j;t_k-t_l|\boldsymbol{\theta})\equiv\text{cov}\{Z(\mathbf{s}_i,t_k),Z(\mathbf{s}_j,t_l)\},\tag{1}$$

where $\mathbf{s}_i=(s_1^i,\cdots,s_d^i)'$ and C satisfies the positive definiteness for all $\boldsymbol{\theta}\in\mathbb{R}^p$. Then the process is called separable if the covariance function in (1) can be divided into a spatial covariance and a temporal one, that is,

$$C(\mathbf{s}_i-\mathbf{s}_j;t_k-t_l|\boldsymbol{\theta})=C_{\mathbf{s}}(\mathbf{s}_i-\mathbf{s}_j|\boldsymbol{\theta}_1)\cdot C_T(t_k-t_l|\boldsymbol{\theta}_2),\tag{2}$$

where $C_{\mathbf{s}}$ is a positive-definite spatial covariance function in $\mathbb{R}^d$, C_T is a positive-definite temporal covariance function in $\mathbb{R}$, and $\boldsymbol{\theta}=(\boldsymbol{\theta}_1',\boldsymbol{\theta}_2')'$. Under the stationarity, (2) is rewritten as

$$C(\mathbf{h};u|\boldsymbol{\theta})=C_{\mathbf{s}}(\mathbf{h}|\boldsymbol{\theta}_1)\cdot C_T(u|\boldsymbol{\theta}_2),\tag{3}$$

for all $\mathbf{h}\equiv(h_1,\cdots,h_d)'=\mathbf{s}_i-\mathbf{s}_j$ and all $u=t_k-t_l$ (see Rodriguez-Iturbe and Majia (1974)). However, in real applications, it may not be reasonable to assume that the covariance function

depends on space and time separately. Especially, for air pollution data, where it is not easy to model the underlying pattern using separable covariance functions. Many reseachers have proposed nonseparable covariance classes for spatial-temporal processes. Jones and Zhang (1997) developed a parametric family of spectral density functions, each of which can be transformed into the corresponding nonseparable stationary covariance function, by adapting stochastic partial differential equations. Cressie and Huang (1999) also introduced new classes of nonseparable, spatial-temporal stationary covariance functions with space-time interaction. Their main idea was to develop the nonseparable positive-definite covariance function with spatial-temporal interaction by specifying two appropriate functions all of which are expressed as their spectral representations in closed form. Gneiting (2002) proposed general classes of nonseparable, stationary spatial-temporal covariance functions which are directly constructed in the space-time domain and are based on Fourier-free implementation. Recently Fuentes *et al.* (2005) introduced a new class of nonseparable covariance models with a unique parameter reflecting the dependency between the spatial and the temporal components. Instead of a covariance function which is the multiplication of spatial and temporal covariances in (3), Rouhani and Hall (1989), and Rouhani and Myers (1990) considered another type of separable model defined as

$$C(\mathbf{s}_i - \mathbf{s}_j; t_k - t_l|\boldsymbol{\theta}) = C_{\mathbf{s}}(\mathbf{s}_i - \mathbf{s}_j|\boldsymbol{\theta}_1) + C_T(t_k - t_l|\boldsymbol{\theta}_2). \tag{4}$$

However, the variance-covariance matrix based on (4) turns out to be singular in some situations where the matrix is the linear combination of the functions each of which only depends on a part of space-time position information (see Myers and Journel (1990)).

The other concept for relieving the difficulty in modeling spatial or spatial-temporal processes is symmetry. This definition orginates from the symmetric property of any variance-covariance matrix, $\Sigma = \{\sigma_{ij}\}_{i,j=1,\cdots,n}$ which always satisfies $\sigma_{ij} = \sigma_{ji}$ for all i and j. Symmetry also has the same advantages as separability. Symmetry plays an important role in helping researchers construct

simplified covariance structures for spatial-temporal processes, and makes easier the interpretation of the underlying characteristics of the processes. Due to these benefits, symmetry is a common assumption. In these days, more attention has been focused on symmetry or lack of symmetry inherent in spatial or spatial-temporal processes although only a few studies have been accomplished so far. One of the noteworthy studies was conducted by Scaccia and Martin (2005), which, for a spatial process, $\{Z(\mathbf{s}) : \mathbf{s} \in \mathbb{D} \subset \mathbb{R}^d\}$, in particular for two-dimensional spatial lattice data, introduced two types of symmetry (axial symmetry; diagonal symmetry) and separability which are, respectively, denoted by, for all h_1 and h_2

$$C(h_1, h_2|\boldsymbol{\theta}_{\mathbf{s}}) = C(-h_1, h_2|\boldsymbol{\theta}_{\mathbf{s}}), \tag{5}$$

$$C(h_1, h_2|\boldsymbol{\theta}_{\mathbf{s}}) = C(h_2, h_1|\boldsymbol{\theta}_{\mathbf{s}}), \tag{6}$$

and

$$C(h_1, h_2|\boldsymbol{\theta}_{\mathbf{s}}) = C_1(h_1|\boldsymbol{\theta}_{\mathbf{s}_1}) \cdot C_2(h_2|\boldsymbol{\theta}_{\mathbf{s}_2}), \tag{7}$$

where C_1 and C_2 are the positive-definite covariances of the corresponding spatial lags, h_1 and h_2, and $\boldsymbol{\theta}_{\mathbf{s}} = \left(\boldsymbol{\theta}'_{\mathbf{s}_1}, \boldsymbol{\theta}'_{\mathbf{s}_2}\right)'$. They also developed new tests for axial symmetry in (5) and separability in (7) based on periodograms. Using ratios of spatial periodograms, Lu and Zimmerman (2005) proposed new diagnostic tests for axial symmetry and complete symmetry, which satisfies both axial symmetry in (5) and diagonal symmetry in (6). However, symmetry has not been adapted yet to the general spatial-temporal setting except Jun and Stein (2004) and Stein (2005), which focused on the covariance models with lack of axial symmetry in time presented in Section 2, but overlooked some useful types of (lack of) symmetry which can be realized in the spatial-temporal processes.

In this study, we classify certain types of symmetry in spatial-temporal processes, and propose new classes of nonseparable spatial-temporal covariance models with spatial-temporal dependency

parameters, which control (lack of) symmetry inherent in the processes. It is one of the advantages that the classes presented in Section 3 are directly derived from simple spectral density functions and, hence, are represented in closed form.

This study is organized as follows. In Section 2, we define three types of symmetry realized in the spatial-temporal setting. Based on the definition of symmetry, we develop new classes of nonseparable covariance models in Section 3. In Section 4, we explain the relationship between assumptions of symmetry and separability for the covariance function, and extend the proposed models to the nonseparable case. In Section 5, we apply our new classes of covariance models to estimate the spatial-temporal structure of Particulate Matter with a mass of median diameter less than $2.5\mu m$ ($PM_{2.5}$) over the northeastern region of U.S. In Section 6, we present some conclusions and final remarks.

2 Symmetry in Spatial-Temporal Processes

In this section, we define three types of symmetry in spatial-temporal processes: 1) axial symmetry in time, 2) axial symmetry in space, and 3) diagonal symmetry in space. For the ease of understanding, we assume that any covariance function in this study is stationary in time defined as, for arbitrary u,

$$\text{cov}\{Z(\mathbf{s}_i, t_k + u), Z(\mathbf{s}_i, t_k)\} = \text{cov}\{Z(\mathbf{s}_i, t_l + u), Z(\mathbf{s}_i, t_l)\},$$

where $\mathbf{s}_i \in \mathbb{D}$ and $t_k,\ t_l \in [0, \infty)$. The first type of symmetry is axial symmetry in time.

Definition 2.1 *A process is called axially symmetric in time if*

$$C(\mathbf{s}_i - \mathbf{s}_j; u) = C(\mathbf{s}_{i^*} - \mathbf{s}_{j^*}; -u), \tag{8}$$

for any temporal lag, $u \neq 0$, and arbitrary four different locations (i, j, i^*, j^*) satisfying $\mathbf{s}_i - \mathbf{s}_j = \mathbf{s}_{i^*} - \mathbf{s}_{j^*}$.

Under stationarity in space, (8) is reduced to

$$C(\mathbf{h}; u) = C(\mathbf{h}; -u), \tag{9}$$

where $\mathbf{s}_i = \mathbf{s}_j + \mathbf{h}$ and $\mathbf{s}_{i^*} = \mathbf{s}_{j^*} + \mathbf{h}$. What is important here is that the directions and the distances on spatial domain are the same, and the temporal lags have the same magnitudes but different signs. The second type of symmetry is axial symmetry in space.

Definition 2.2 *A process is called axially symmetric in space if*

$$C(\mathbf{h}; u) = C(\mathring{\mathbf{h}}; u), \tag{10}$$

where $\mathring{\mathbf{h}} = (h_1, \cdots, h_{k-1}, -h_k, h_{k+1}, \cdots, h_d)'$ *for* k *fixed.*

As can be seen in (10), for temporal lag u fixed, all the spatial lags are the same except one spatial lag, which has different sign. The last one is diagonal symmetry in space.

Definition 2.3 *A process is called diagonally symmetric in space if*

$$C(\mathbf{h}; u) = C(\ddot{\mathbf{h}}; u), \tag{11}$$

where $\ddot{\mathbf{h}} = (h_1, \cdots, h_{k-1}, h_l, h_{k+1}, \cdots, h_{l-1}, h_k, h_{l+1}, \cdots, h_d)'$ *for* $k \neq l$.

From (11) we can see that only two spatial lags, h_k and h_l, are switched with each other.

A process which satisfies none of the three types of symmetry is called asymmetric in space and time, or lacking symmetry in space and time.

3 Classes of Asymmetric Stationary Covariance Models

In Section 2, we defined three different types of symmetry inherent in covariance function of spatial-temporal processes. From (10) and (11) one can simply expect that $\mathring{\mathbf{h}} = (h_1, -h_2)'$ and $\ddot{\mathbf{h}} = (h_2, h_1)'$. In general, these may or may not hold in the real applications, especially in the analysis

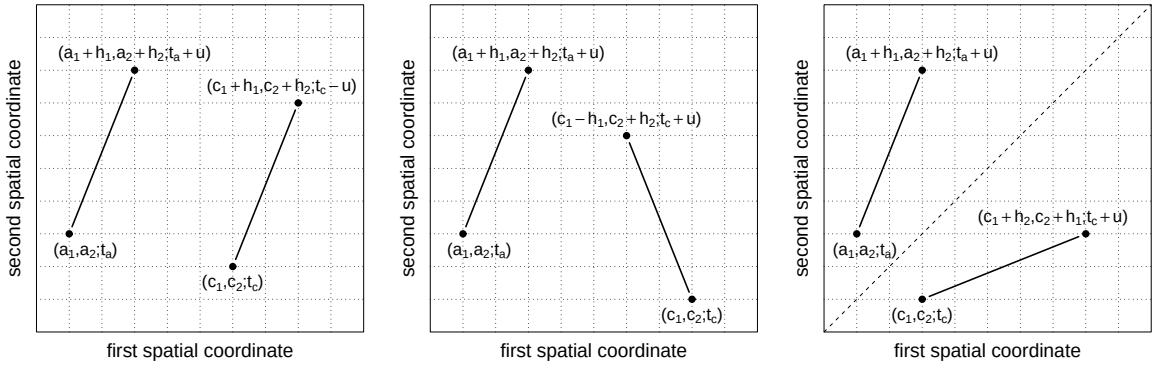

(a) (b) (c)

Figure 1: Visualizations of the definitions of symmetry in a spatial-temporal process. (a) axial symmetry in time; (b) axial symmetry in space; (c) diagonal symmetry in space.

of environmental data. Suppose that we have air-pollution data with the covariance structure presented in (1). From Figure 1(a) displaying axial symmetry in time, the relationship between $Z(\mathbf{a}; t_a)$ and $Z(\mathbf{a}+\mathbf{h}; t_a+u)$ may not be similar to the one between $Z(\mathbf{c}; t_c)$ and $Z(\mathbf{c}+\mathbf{h}; t_c-u)$ where $\mathbf{a} = (a_1, a_2)'$, $\mathbf{c} = (c_1, c_2)'$ and $\mathbf{h} = (h_1, h_2)'$. The dissimilarity may result from the changes of meteorological conditions, for example, temperature, humidity, wind direction and so on. The other definitions may be also unreasonable in the real applications even though the process always has symmetric property of the variance-covariance matrix. We consider wind speed measurements during hurricane season as an example for the better undestanding of diagonal symmetry in space. Provided that a hurricane track moves along the dashed line in Figure 1(c), it is well known that the wind speed measured at sites in upper-left region is different from the one at sites in lower-right region. This phenomenon results in lack of diagonal symmetry in space. These examples frequently faced in the environmental research fields encourage us to take lack of symmetry into account.

In this section, we propose new classes of asymmetric spatial-temporal stationary covariance models wherein stationarity both in time and in space is assumed. Now we provide a new and

simple method to construct such covariance models. The main idea of our approach is to build covariance functions directly derived from simple spectral density functions. Before going further, we briefly talk about spectral density functions. A stationary spatial-temporal process $\{Z(\mathbf{s};t) : \mathbf{s} \in \mathbb{D} \subset \mathbb{R}^d,\ t \in [0,\infty)\}$ can be represented in the spectral domain by using sinusoidal forms with different frequencies $(\boldsymbol{\omega}, \tau)$, where $\boldsymbol{\omega}$ is d-dimensional spatial frequency, and τ is temporal frequency. If $Z(\mathbf{s},t)$ is a stationary spatial-temporal process with the corresponding covariance $C(\mathbf{h};u)$, then we can rewrite the process in the following Fourier-Stieltjes integral (see Yaglom (1987)):

$$Z(\mathbf{s},t) = \int_{\mathbb{R}^d}\int_{\mathbb{R}} \exp\{i\mathbf{s}'\boldsymbol{\omega} + i\tau t\}\ dY(\boldsymbol{\omega},\tau),$$

where Y is a random process with complex symmetry except for the constraint, $dY(\boldsymbol{\omega},\tau) = dY^c(-\boldsymbol{\omega},-\tau)$, which ensures that $Z(\mathbf{s},t)$ is real-valued. Using the spectral representation of Z, the covariance function $C(\mathbf{h};u)$ can be represented as

$$C(\mathbf{h};u) = \int_{\mathbb{R}^d}\int_{\mathbb{R}} \exp\{i\mathbf{h}'\boldsymbol{\omega} + iu\tau\}\ F(d\boldsymbol{\omega}, d\tau), \tag{12}$$

where the function F is a positive finite measure called the spectral measure or spectrum for Z. The spectral measure F is the expected squared modulus of the process Y denoted by

$$E\left\{|Y(\boldsymbol{\omega},\tau)|^2\right\} = F(\boldsymbol{\omega},\tau).$$

We can easily see that $C(\mathbf{h};u)$ in (12) is always positive-definite for any finite positive measure F. If F has a density with respect to Lebesgue measure, the spectral density f is the Fourier transform of the spatial-temporal covariance function denoted as

$$f(\boldsymbol{\omega},\tau) = \frac{1}{(2\pi)^{d+1}}\int_{\mathbb{R}}\int_{\mathbb{R}^d} \exp\{-i\mathbf{h}'\boldsymbol{\omega} - iu\tau\}C(\mathbf{h};u)\ d\mathbf{h}\ du, \tag{13}$$

and the corresponding covariance function is given by

$$C(\mathbf{h};u) = \int_{\mathbb{R}}\int_{\mathbb{R}^d} \exp\{i\mathbf{h}'\boldsymbol{\omega} + iu\tau\}\ f(\boldsymbol{\omega},\tau)\ d\boldsymbol{\omega}\ d\tau. \tag{14}$$

Based on the relationship between (13) and (14), we propose the spatial-temporal spectral density function given by

$$\begin{aligned} f_{\mathbf{v}}(\boldsymbol{\omega};\tau) &= \gamma\left(\alpha^2\beta^2 + \beta^2\|\boldsymbol{\omega}+\tau\mathbf{v}_1\|^2 + \alpha^2(\tau+\mathbf{v}_2'\boldsymbol{\omega})^2\right)^{-\nu} \\ &= f_0(\boldsymbol{\omega}+\tau\mathbf{v}_1;\tau+\mathbf{v}_2'\boldsymbol{\omega}), \end{aligned} \tag{15}$$

where $\|\cdot\|$ denotes the Euclidean distance, $f_0(\boldsymbol{\omega};\tau) \equiv \gamma(\alpha^2\beta^2+\beta^2\|\boldsymbol{\omega}\|^2+\alpha^2\tau^2)^{-\nu}$ is a simple spectral density function, γ, α and β are positive, $\nu > \frac{d+1}{2}$, and $|\mathbf{v}_1'\mathbf{v}_2| < 1$. Here $\mathbf{v}_1 = (v_{11},\cdots,v_{1d})'$ and $\mathbf{v}_2 = (v_{21}\cdots,v_{2d})'$ are vectors controling certain types of (lack of) symmetry. The spectral density function in (15) is always valid because , for all $\mathbf{v}_1,\ \mathbf{v}_2 \in \mathbb{R}^d$ with $|\mathbf{v}_1'\mathbf{v}_2| < 1$, $0 < f_{\mathbf{v}}(\boldsymbol{\omega};\tau) < \infty$, and, therefore, its Fourier transformation always exists. So, the corresponding covariance function,

$$C_{\mathbf{v}}(\mathbf{h};u) = \int_{\mathbb{R}^d}\int_{\mathbb{R}} \exp\{i\mathbf{h}'\boldsymbol{\omega}+iu\tau\} f_{\mathbf{v}}(\boldsymbol{\omega};\tau)\, d\tau\, d\boldsymbol{\omega}$$

exists and has the positive-definiteness. We can write the covariance function derived from the spectral density function, $f_{\mathbf{v}}$ in (15) as

$$\begin{aligned} C_{\mathbf{v}}(\mathbf{h};u) &= \int_{\mathbb{R}^d}\int_{\mathbb{R}} \exp\{i\mathbf{h}'\boldsymbol{\omega}+iu\tau\} f_0(\boldsymbol{\omega}+\tau\mathbf{v}_1;\tau+\mathbf{v}_2'\boldsymbol{\omega})\, d\tau\, d\boldsymbol{\omega} \\ &= \int_{\mathbb{R}^d}\int_{\mathbb{R}} \exp\left\{ i\frac{(\widetilde{\mathbf{h}}-u\mathbf{v}_2)'}{1-\mathbf{v}_1'\mathbf{v}_2}\boldsymbol{\omega} + i\frac{(u-\mathbf{h}'\mathbf{v}_1)}{1-\mathbf{v}_1'\mathbf{v}_2}\tau \right\} \frac{f_0(\boldsymbol{\omega};\tau)}{1-\mathbf{v}_1'\mathbf{v}_2}\, d\tau\, d\boldsymbol{\omega} \\ &= \frac{1}{1-\mathbf{v}_1'\mathbf{v}_2}\, C_0\left(\frac{\widetilde{\mathbf{h}}-u\mathbf{v}_2}{1-\mathbf{v}_1'\mathbf{v}_2}; \frac{u-\mathbf{h}'\mathbf{v}_1}{1-\mathbf{v}_1'\mathbf{v}_2}\right), \end{aligned} \tag{16}$$

where C_0 is a stationary spatial-temporal covariance function simply transformed from f_0, and $\widetilde{\mathbf{h}} = \left(\widetilde{h}_1,\cdots,\widetilde{h}_d\right)'$, where

$$\widetilde{h}_i \equiv \left(1-\sum_{j\neq i}^{d} v_{1j}v_{2j}\right) h_i + v_{2i}\sum_{j\neq i}^{d} v_{1j}h_j.$$

By straightforward derivation with help of Stein (2005), and Gradshteyn and Ryzhik (2000) (see Appendix), we finally obtain the closed form of the $(d+1)$ dimensional asymmetric stationary

Matérn-type covariance function denoted by

$$C_{\mathbf{v}}(\mathbf{h};u) = \frac{1}{1-\mathbf{v}_1'\mathbf{v}_2} \times \frac{\gamma\pi^{(d+1)/2}\alpha^{-2\nu+d}\beta^{-2\nu+1}}{2^{\nu-(d+1)/2-1}\Gamma(\nu)} \times \mathcal{M}_{\nu-\frac{d+1}{2}}\left(\sqrt{\left\{\frac{\alpha\|\widetilde{\mathbf{h}}-u\mathbf{v}_2\|}{1-\mathbf{v}_1'\mathbf{v}_2}\right\}^2+\left\{\frac{\beta(u-\mathbf{h}'\mathbf{v}_1)}{1-\mathbf{v}_1'\mathbf{v}_2}\right\}^2}\right), \tag{17}$$

where $\mathcal{M}_\nu(r) \equiv r^\nu\mathcal{K}_\nu(r)$ and $\mathcal{K}_\nu$ is a modified Bessel function of the third kind of order ν. The parameters, α and β explain the decaying rates of the spatial and the temporal correlations ($0 < \alpha, \beta \leq 1$). So their inverses are interpreted as the spatial and the temporal ranges. ν measures the degree of smoothness, which means that the larger the ν is, the smoother a process is. What is important here is the spatial-temporal dependency parameter vectors or asymmetry vectors, $\mathbf{v}_1$ and $\mathbf{v}_2$. From (16) and (17), both the temporal component, $u - \mathbf{h}'\mathbf{v}_1$, and the spatial component, $\widetilde{\mathbf{h}} - u\mathbf{v}_2$ are adjusted by u and $\mathbf{h}$ under the control of the asymmetry vectors, $\mathbf{v}_1$ and $\mathbf{v}_2$. The asymmetry vectors, $\mathbf{v}_1$ and $\mathbf{v}_2$ measure the inverse of speeds and the velocities, respectively, in that $\mathbf{v}_1$ is a temporal adjustment by spatial distance and $\mathbf{v}_2$ is a spatial adjustment by temporal lag. These asymmetry vectors play an important role in developing new classes of asymmetric covariance models and, for $d = 2$, yield the covariance models with the following types of symmetry:

T.1 axial symmetry in time if $\mathbf{v}_1 = \mathbf{v}_2 = \mathbf{0}$,

T.2 axial symmetry in space if $v_{11} \neq 0$ or $v_{21} \neq 0$ and $v_{12} = v_{22} = 0$,

T.3 diagonal symmetry in space if $v_{11} = v_{12} = v_{10}$, $v_{21} = v_{22} = v_{20}$,
and at least one of v_{10} and v_{20} is nonzero,

T.4 asymmetry in space and time otherwise.

This classification of symmetry based on the asymmetry vectors provides the fact that all types of symmetry here are exclusive with one another. For the simplification of an asymmetric covariance

function in (17), we can consider, as special cases, the two covariance models as follow:

$$C_{\mathbf{v}_1}(\mathbf{h};u) = \frac{\gamma\pi^{(d+1)/2}\alpha^{-2\nu+d}\beta^{-2\nu+1}}{2^{\nu-(d+1)/2-1}\Gamma(\nu)}\mathcal{M}_{\nu-\frac{d+1}{2}}\left(\alpha\sqrt{\left\{\frac{\beta(u-\mathbf{h}'\mathbf{v}_1)}{\alpha}\right\}^2+\|\mathbf{h}\|^2}\right), \tag{18}$$

and

$$C_{\mathbf{v}_2}(\mathbf{h};u) = \frac{\gamma\pi^{(d+1)/2}\alpha^{-2\nu+d}\beta^{-2\nu+1}}{2^{\nu-(d+1)/2-1}\Gamma(\nu)}\mathcal{M}_{\nu-\frac{d+1}{2}}\left(\alpha\sqrt{\left(\frac{\beta u}{\alpha}\right)^2+\|\mathbf{h}-u\mathbf{v}_2\|^2}\right). \tag{19}$$

The corresponding spectral density functions are, respectively, given by

$$f_{\mathbf{v}_1}(\boldsymbol{\omega};\tau) = \gamma\left(\alpha^2\beta^2+\beta^2\|\boldsymbol{\omega}+\tau\mathbf{v}_1\|^2+\alpha^2\tau^2\right)^{-\nu}, \tag{20}$$

and

$$f_{\mathbf{v}_2}(\boldsymbol{\omega};\tau) = \gamma\left(\alpha^2\beta^2+\beta^2\|\boldsymbol{\omega}\|^2+\alpha^2(\tau+\mathbf{v}_2'\boldsymbol{\omega})^2\right)^{-\nu}. \tag{21}$$

It is certain that both $f_{\mathbf{v}_1}(\boldsymbol{\omega};\tau)$ and $f_{\mathbf{v}_2}(\boldsymbol{\omega};\tau)$ are valid, so the corresponding covariance functions in (18) and (19) are always positive-definite.

Now we present the characteristics of an asymmetric stationary covariance function in (17) derived from (15). The parameters are set to $\gamma = 1$, $\nu = d = 2$, $\alpha = 0.02$ and $\beta = 1$ unless mentioned otherwise. Figure 2 displays the behaviors of a spatial-temporal covariance function axially symmetric in time, and shows that, under axial symmetry in time, the covariance function does not change whatever $\mathbf{h}$ and u are (Figure 2(a), (b)). The parameters, α and β changes the shape of covariance function (Figure 2(c)). Figure 3 shows that the pattern of a covariance axially symmetric in space depends on the temporal lag, u as well as the spatial lag, h_1. This implies that the covariance function moves along the axes of the spatial lag, h_1 and the temporal lag, u as h_1 and u change, and the direction and the speed of movement really depend on the sign and the magnitude of the asymmetry vector, $\mathbf{v}$ (Figure 3(a), (c)). For instance, in case that $\max(v_{11}, v_{21}) > 0$ and $v_{11}v_{21} \geq 0$, the covariance moves in the same direction as h_1 increases (Figure 3(a)) and u increases

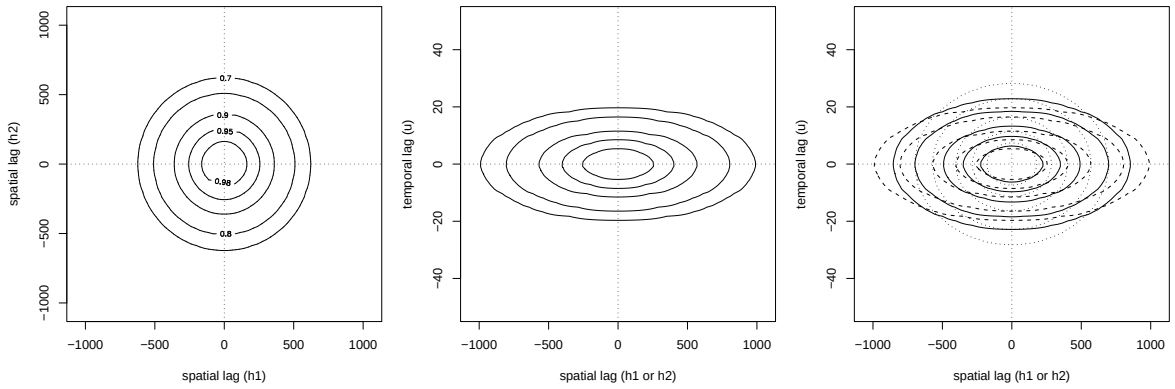

(a) (b) (c)

Figure 2: Contour plots for $C_{\mathbf{v}}(\mathbf{h}; u)$ axially symmetric in time ($\mathbf{v}_1 = \mathbf{v}_2 = \mathbf{0}$), where each number in plot indicates the corresponding percentile of the covariance. (a) $C_{\mathbf{v}}(\mathbf{h}; u)$ versus h_1 and h_2 for all u; (b) $C_{\mathbf{v}}(\mathbf{h}; u)$ versus h_1 (or h_2) and u; (c) $C_{\mathbf{v}}(\mathbf{h}; u)$ with $\beta = 0.5, 0.75, 1$. Dotted line is for the first case, solid line for the second, and dashed line for the third.

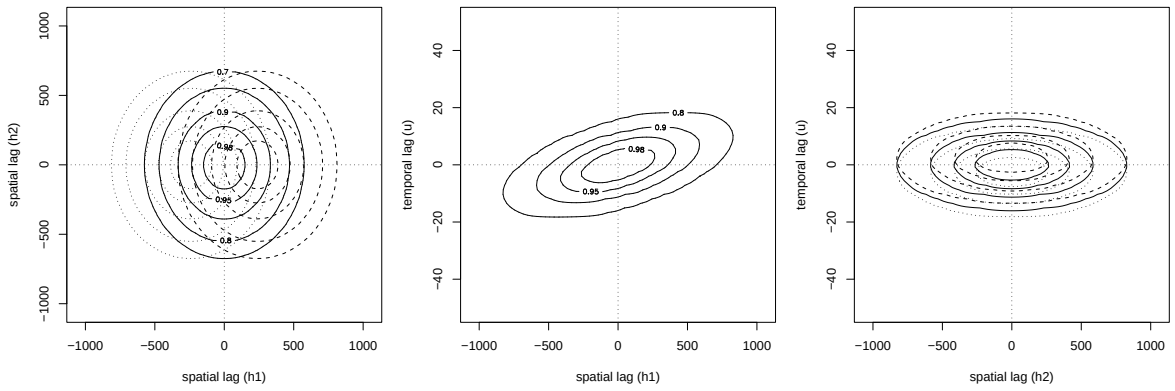

(a) (b) (c)

Figure 3: Contour plots for $C_{\mathbf{v}}(\mathbf{h}; u)$ axially symmetric in space ($\mathbf{v}_1 = (0.01, 0)'$ and $\mathbf{v}_2 = (5, 0)'$). (a) $C_{\mathbf{v}}(\mathbf{h}; u)$ versus h_1 and h_2 for $u = -10, 0, 10$; (b) $C_{\mathbf{v}}(\mathbf{h}; u)$ versus h_1 and u for all h_2; (c) $C_{\mathbf{v}}(\mathbf{h}; u)$ versus h_2 and u for $h_1 = -200, 0, 200$.

(Figure 3(c)). However, if $\max(v_{11}, v_{21}) > 0$ but $v_{11}v_{21} < 0$, then the direction and the speed are determined by the contributions from the spatial component, $\alpha\|\widetilde{\mathbf{h}} - u\mathbf{v}_2\|$, and from the temporal component, $\beta|u - \mathbf{h}'\mathbf{v}_1|$. Figure 3(b) provides the information that the components, $\alpha\|\widetilde{\mathbf{h}} - u\mathbf{v}_2\|$ and $\beta|u - \mathbf{h}'\mathbf{v}_1|$ have no effect of the spatial lag, h_2 because $v_{12} = v_{22} = 0$, and the decaying rates as well as the asymmetry vectors controls the obliqueness and the shape of the covariance function. Figure 4 displays the behavior of the covariance function diagonally symmetric in space. Unlike the covariance function axially symmetric in space, this covariance moves along the diagonal dotted line ($h_1 = h_2$) (Figure 4(a)) and along with the axis of u (Figure 4(b)). This type of symmetry can be applicable to the case that the movement is on the line that $h_1 = k \cdot h_2$, where k is a known constant. The asymmetry vectors along with the decaying rates also control the shape of the covariance (Figure 4(c)). Figure 5 displayes the patterns of a covariance function which is

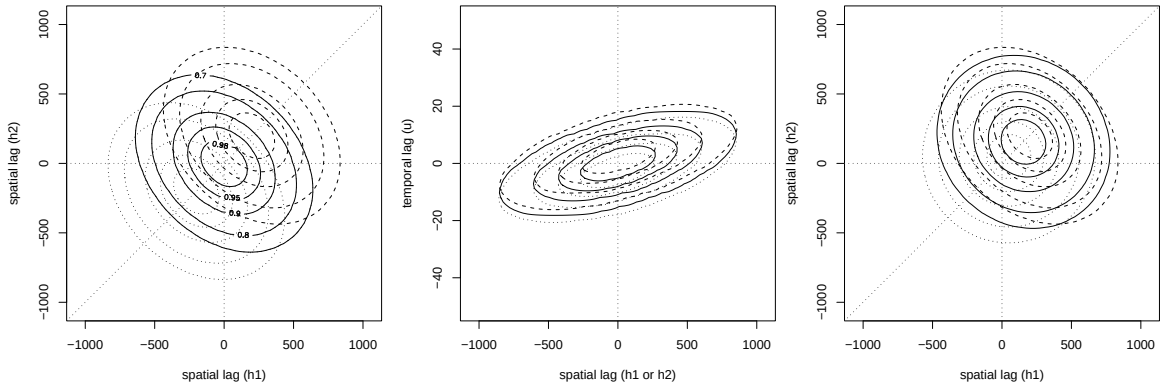

(a) (b) (c)

Figure 4: Contour plots for $C_{\mathbf{v}}(\mathbf{h}; u)$ digonally symmetric in space ($v_{10} = 0.01$ and $v_{20} = 5$). (a) $C_{\mathbf{v}}(\mathbf{h}; u)$ versus h_1 and h_2 for $u = -10, 0, 10$; (b) $C_{\mathbf{v}}(\mathbf{h}; u)$ versus h_1 (or h_2) and u for h_2 (h_1)$= -200, 0, 200$; (c) $C_{\mathbf{v}}(\mathbf{h}; u)$ versus h_1 and h_2 for $v_{10} = 0, 0.005, 0.01$ and $u = 10$.

asymmetric in space and time. For simplifing the covariance structure, we only consider the case that $\mathbf{v}_2 = \mathbf{0}$. Figure 5 shows that the covariance moves along the line that $h_1 = k(\mathbf{v}, \alpha, \beta) \cdot h_2$ where

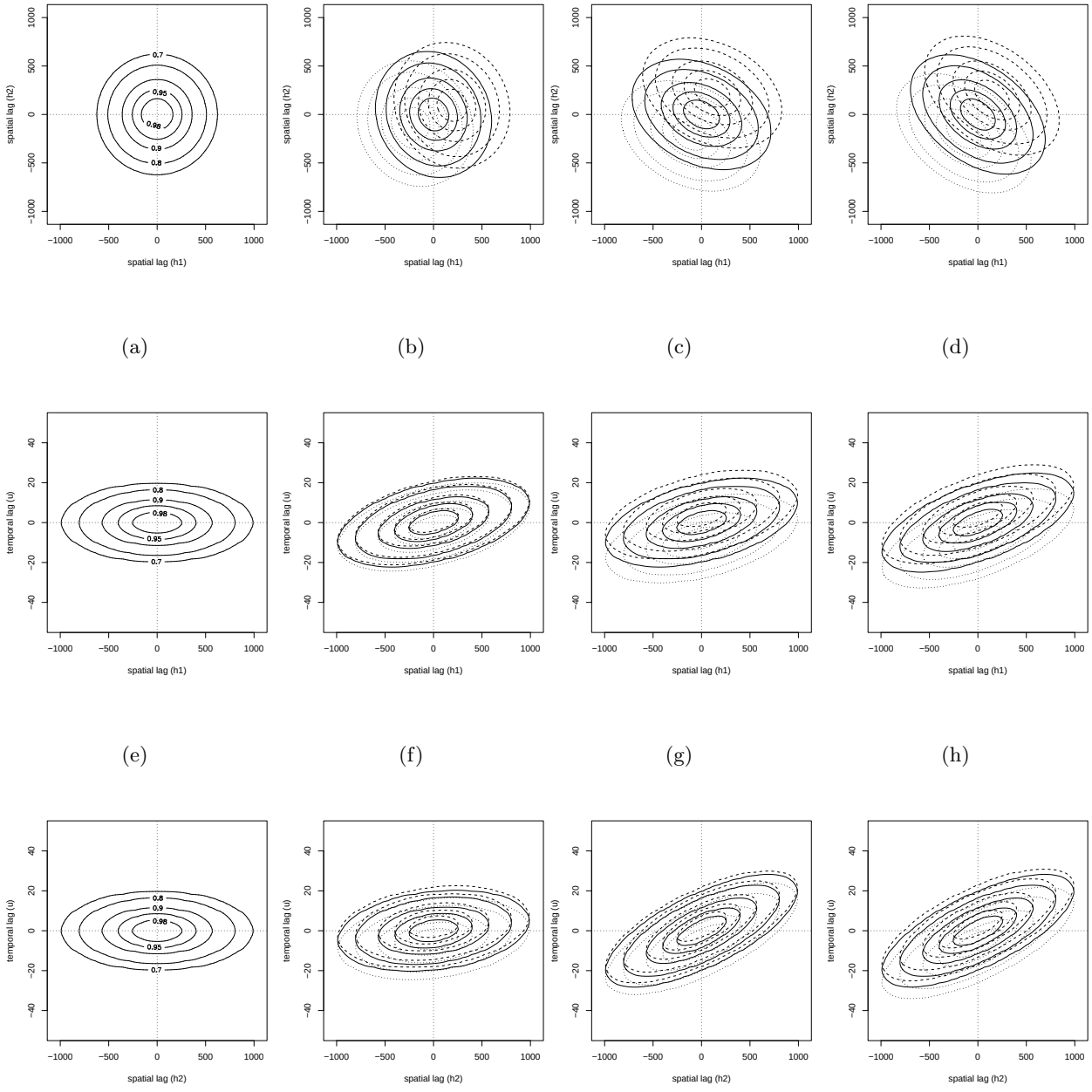

(a) (b) (c) (d)

(e) (f) (g) (h)

(i) (j) (k) (l)

Figure 5: Contour plots for $C_{\mathbf{v}}(\mathbf{h}; u)$ asymmetric in space and time. (a) – (d) $C_{\mathbf{v}}(\mathbf{h}; u)$ versus h_1 and h_2 for $u = -10, 0, 10$; (e) – (h) $C_{\mathbf{v}}(\mathbf{h}; u)$ versus h_1 and u for $h_2 = -400, 0, 400$; (i) – (l) $C_{\mathbf{v}}(\mathbf{h}; u)$ versus h_2 and u for $h_1 = -400, 0, 400$. (a)(e)(i) $\mathbf{v}_1 = (0, 0)'$; (b)(f)(j) $\mathbf{v}_1 = (0.01, 0.005)'$; (c)(g)(k) $\mathbf{v}_1 = (0.01, 0.02)'$; (d)(h)(l) $\mathbf{v}_1 = (0.015, 0.02)'$.

$k(\mathbf{v}, \alpha, \beta)$ is a function based on the asymmetry vectors and the decaying rates, and the features of the covariance are directly influenced by them (Figure 5(a) – (d)). This figure also demonstrates that, in terms of each of spatial lags, the covariance moves along the axis of u at different speed, which is controled by the magnitude of the corresponding element in $\mathbf{v}$.

In this section, we have proposed new classes of asymmetric spatial-temporal covariance models by using a simple and valid spectral density function, which guarantees the positive-definiteness of the corresponding covariance function. Symmetry or lack of symmetry are controled by the asymmetry parameter vectors, $\mathbf{v}_1$ and $\mathbf{v}_2$ in that magnitude and sign of each element are quitely related to the direction and the speed of movement in the modeled field. They also play an important role in changing features of the covariance functions. However, the interpretation of asymmetry vectors are different in that the units of $\mathbf{v}_1$ are time divided by distances, that is, the reciprocals of speed whereas the units of $\mathbf{v}_2$ are distances divided by time (velocities).

4 Symmetry and Separability

In this section, we clarify the relationship between symmetry and separability in spatial-temporal processes and, based on a separable spectral density function, extend the models proposed in Section 3 to the nonseparable case. Symmetry and separability are the main assumptions about the covariance function that are frequently applied to most applications in the environmental research. The common advantage of the assumptions of symmetry and separability is the simplification attained for modeling purpose.

Taking symmetry as well as separability into account, we now propose another new class of asymmetric spatial-temporal stationary covariance models, in which separable one is a special case. In order to build the covariance functions asymmetric as well as nonseparable, we consider the

following spectral density function:

$$\begin{aligned} f_{\mathbf{v}}(\boldsymbol{\omega};\tau) &= \gamma\left(\alpha^2+\|\boldsymbol{\omega}+\tau\mathbf{v}_1\|^2\right)^{-\nu}\left(\beta^2+(\tau+\mathbf{v}_2'\boldsymbol{\omega})^2\right)^{-\nu} \\ &= f_0(\boldsymbol{\omega}+\tau\mathbf{v}_1;\tau+\mathbf{v}_2'\boldsymbol{\omega}), \end{aligned} \tag{22}$$

where $f_0(\boldsymbol{\omega};\tau)\equiv\gamma\left(\alpha^2+\|\boldsymbol{\omega}\|^2\right)^{-\nu}\left(\beta^2+\tau^2\right)^{-\nu}$ is the spectral density function transformed from a stationary separable covariance function. Based on the setting of (22), we can express the corresponding covariance function as

$$\begin{aligned} C_{\mathbf{v}}(\mathbf{h};u) &= \int_{\mathbb{R}^d}\int_{\mathbb{R}}\exp\{i\mathbf{h}'\boldsymbol{\omega}+iu\tau\}f_0(\boldsymbol{\omega}+\tau\mathbf{v}_1;\tau+\mathbf{v}_2'\boldsymbol{\omega})\,d\tau\,d\boldsymbol{\omega} \\ &= \int_{\mathbb{R}^d}\int_{\mathbb{R}}\exp\left\{i\frac{(\widetilde{\mathbf{h}}-u\mathbf{v}_2)'}{1-\mathbf{v}_1'\mathbf{v}_2}\boldsymbol{\omega}+i\frac{(u-\mathbf{h}'\mathbf{v}_1)}{1-\mathbf{v}_1'\mathbf{v}_2}\tau\right\}\frac{f_0(\boldsymbol{\omega};\tau)}{1-\mathbf{v}_1'\mathbf{v}_2}\,d\tau\,d\boldsymbol{\omega} \\ &= \frac{1}{1-\mathbf{v}_1'\mathbf{v}_2}\,C_{\mathbf{s}}\left(\frac{\widetilde{\mathbf{h}}-u\mathbf{v}_2}{1-\mathbf{v}_1'\mathbf{v}_2}\right)C_T\left(\frac{u-\mathbf{h}'\mathbf{v}_1}{1-\mathbf{v}_1'\mathbf{v}_2}\right), \end{aligned} \tag{23}$$

where $C_{\mathbf{s}}$ is a two-dimensional spatial covariance function and C_T is an one-dimensional temporal covariance function. By direct derivation from (23) (see Stein (2005)), we can obtain the closed form of the asymmetric nonseparable covariance function given by

$$\begin{aligned} C_{\mathbf{v}}(\mathbf{h};u) =& \frac{1}{1-\mathbf{v}_1'\mathbf{v}_2}\times\frac{\gamma\pi^{(d+1)/2}\alpha^{-2\nu+d}\beta^{-2\nu+1}}{2^{\nu-(d+1)/2-2}\Gamma^2(\nu)} \\ &\times\mathcal{M}_{\nu-d/2}\left(\alpha\left\|\frac{\widetilde{\mathbf{h}}-u\mathbf{v}_2}{1-\mathbf{v}_1'\mathbf{v}_2}\right\|\right)\mathcal{M}_{\nu-1/2}\left(\beta\left|\frac{u-\mathbf{h}'\mathbf{v}_1}{1-\mathbf{v}_1'\mathbf{v}_2}\right|\right). \end{aligned} \tag{24}$$

From (24), we know that the asymmetry vectors $\mathbf{v}_1$ and $\mathbf{v}_2$ control separability as well as symmetry. Under the setting of (23), the following types of symmetry are classified:

T.1* axial symmetry in time and separable if $\mathbf{v}_1=\mathbf{v}_2=\mathbf{0}$,

T.2* axial symmetry in space but nonseparable if $v_{11}\neq 0$ or $v_{21}\neq 0$ and $v_{12}=v_{22}=0$,

T.3* diagonal symmetry in space but nonseparable if $v_{11}=v_{12}=v_{10}$, $v_{21}=v_{22}=v_{20}$, and at least one of v_{10} and v_{20} is nonzero,

T.4* asymmetry in space and time, and nonseparable otherwise.

The main difference between the two asymmetric covariance models, (16) and (23) is whether separable covariance model is a particular case or not. That is, (16) is always nonseparable for all posssible $\mathbf{v} \in \mathbb{R}^d$ whereas (23) can be separable (see **T.1***). Similarly, we consider the following two asymmetric nonseparable spatial-temporal covariance models:

$$C_{\mathbf{v}_1}(\mathbf{h};u) = \frac{\gamma\pi^{(d+1)/2}\alpha^{-2\nu+d}\beta^{-2\nu+1}}{2^{\nu-(d+1)/2-2}\Gamma^2(\nu)}\mathcal{M}_{\nu-d/2}\left(\alpha\|\mathbf{h}\|\right)\mathcal{M}_{\nu-1/2}\left(\beta|u-\mathbf{h}'\mathbf{v}_1|\right), \tag{25}$$

and

$$C_{\mathbf{v}_2}(\mathbf{h};u) = \frac{\gamma\pi^{(d+1)/2}\alpha^{-2\nu+d}\beta^{-2\nu+1}}{2^{\nu-(d+1)/2-2}\Gamma^2(\nu)}\mathcal{M}_{\nu-d/2}\left(\alpha\|\mathbf{h}-u\mathbf{v}_2\|\right)\mathcal{M}_{\nu-1/2}\left(\beta|u|\right). \tag{26}$$

The corresponding spectral density functions are, respectively, given by

$$f_{\mathbf{v}_1}(\boldsymbol{\omega};\tau) = \gamma\left(\alpha^2+\|\boldsymbol{\omega}+\tau\mathbf{v}_1\|^2\right)^{-\nu}\left(\beta^2+\tau^2\right)^{-\nu}, \tag{27}$$

and

$$f_{\mathbf{v}_2}(\boldsymbol{\omega};\tau) = \gamma\left(\alpha^2+\|\boldsymbol{\omega}\|^2\right)^{-\nu}\left(\beta^2+(\tau+\mathbf{v}_2'\boldsymbol{\omega})^2\right)^{-\nu}. \tag{28}$$

In this section, we combined symmetry and separability inherent in spatial-temporal processes, and create an alternative class of asymmetric nonseparable spatial-temporal stationary covariance models, which can be extended to nonstationary case.

5 Application to Air Pollution

In this section, we apply the class of asymmetric stationary spatial-temporal covariance models introduced in this paper to an air-pollution dataset with daily fine Particulate Matter ($PM_{2.5}$) daily concentrations obtained from the U.S. Environmental Protection Agency (EPA)'s Federal Reference Method (FRM) monitoring stations and compare asymmetric models with asymmetric one in terms of spatial and temporal prediction. The geographic domain used for our analysis is

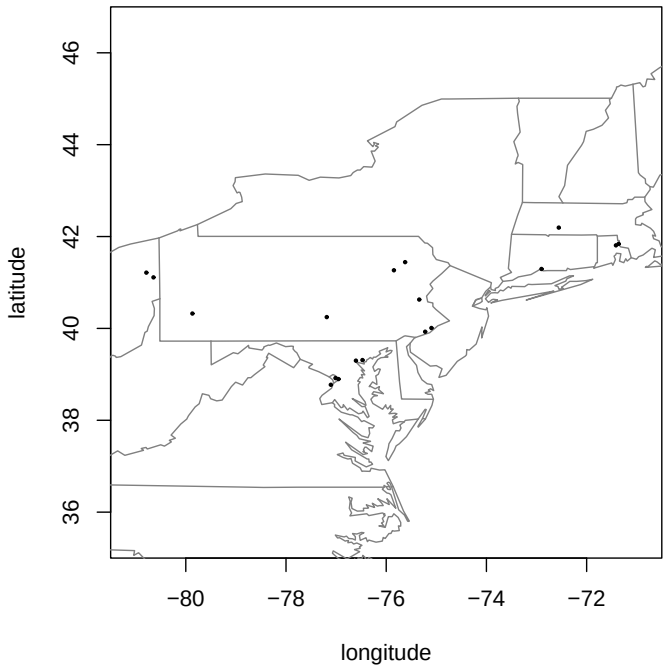

Figure 6: The map of the 18 monitoring stations in the northeastern U.S.

shown in Figure 6, where the 18 monitoring stations were selected among 62 stations located in the eastern U.S by the cluster analysis for relieving nonstationarity problem in space domain. The measurements were obtained from August 1st to August 31st, 2003. The main reason why we are interested in $PM_{2.5}$ concentrations is that exposure to small particles such as PM_{10} and $PM_{2.5}$ results in a variety of adverse health effects. Especially, $PM_{2.5}$ is considered to have more serious effects than PM_{10} due to the smaller size, particularly for the respiratory or the cardiovascular systems. So, the effect of $PM_{2.5}$ have been one of main concerns in the public health (see Zidek (1997) and Golam Kibria *et al.* (2002)).

Now we briefly introduce the weighted least squares (WLS) estimation method which can be applied to asymmetric spatial-temporal covariance models. Let $Z(\mathbf{s}_i, t)$ be the observed $PM_{2.5}$ concentration for time t at site i; $t = 1, \cdots, T(= 31)$, $i = 1, \cdots, N(= 18)$, and $X(\mathbf{s})$ and $Y(\mathbf{s})$ be the geodesic distances with unit of kilometers. Then we consider the spatial-temporal structure as

follows:

$$Z(\mathbf{s}_i, t) = g(X(\mathbf{s}_i), Y(\mathbf{s}_i)|\boldsymbol{\delta}) + \epsilon(\mathbf{s}_i, t),$$

where g is the second-order polynomial function with coefficient parameters $\boldsymbol{\delta}$, $\boldsymbol{\epsilon} \sim MN(\mathbf{0}, \sigma\mathbf{I} + \boldsymbol{\Sigma}(\boldsymbol{\theta}))$, σ is the nugget effect, and $\boldsymbol{\theta} = (\phi, \alpha, \beta, \mathbf{v}_1', \mathbf{v}_2')'$, where ϕ is the partial sill. The variance-covariance matrix of the error vector $\boldsymbol{\epsilon}$ is based on the following Exponential covariance functions:

M.1 $C_0(\mathbf{h}; u) = \phi \exp\left\{\sqrt{\alpha^2\|\mathbf{h}\|^2 + \beta^2 u^2}\right\} + \sigma I_{(\mathbf{h}=\mathbf{0};u=0)}$

M.2 $C_{\mathbf{v}_1}(\mathbf{h}; u) = \phi \exp\left\{\sqrt{\alpha^2\|\mathbf{h}\|^2 + \beta^2(u - \mathbf{v}_1'\mathbf{h})^2}\right\} + \sigma I_{(\mathbf{h}=\mathbf{0};u=0)}$

M.3 $C_{\mathbf{v}_2}(\mathbf{h}; u) = \phi \exp\left\{\sqrt{\alpha^2\|\mathbf{h} - u\mathbf{v}_2\|^2 + \beta^2 u^2}\right\} + \sigma I_{(\mathbf{h}=\mathbf{0};u=0)}$

M.4 $C_{\mathbf{v}}(\mathbf{h}; u) = \dfrac{\phi}{1 - \mathbf{v}_1'\mathbf{v}_2} \exp\left\{\dfrac{\sqrt{\alpha^2\|\widetilde{\mathbf{h}} - u\mathbf{v}_2\|^2 + \beta^2(u - \mathbf{v}_1'\mathbf{h})^2}}{1 - \mathbf{v}_1'\mathbf{v}_2}\right\} + \sigma I_{(\mathbf{h}=\mathbf{0};u=0)}.$

Here $I_{(\cdot)}$ is an indicator function. In order to estimate the covariance parameters, $\boldsymbol{\Theta} = (\sigma, \boldsymbol{\theta}')'$, we propose the empirical spatial-temporal semivariogram, $\widehat{\gamma}(\mathbf{h}(p,q); u)$ given by

$$\widehat{\gamma}(\mathbf{h}(p,q); u) \equiv \frac{1}{N(\mathbf{h}(p,q); u)} \sum_{(i,j,t,t^*) \in N(\mathbf{h}(p,q);u)} \left(\widetilde{Z}(\mathbf{s}_i, t) - \widetilde{Z}(\mathbf{s}_j, t^*)\right)^2, \tag{29}$$

where

$$N(\mathbf{h}(p,q); u) \equiv \left\{(i,j,t,t^*) : \left|s_1^i - s_1^j\right| \in \mathcal{T}_1(\mathbf{h}(p,q)); \left|s_2^i - s_2^j\right| \in \mathcal{T}_2(\mathbf{h}(p,q)); |t - t^*| = u\right\}, \tag{30}$$

and $\widetilde{Z}(\mathbf{s}, t) = Z(\mathbf{s}, t) - g\left(X(\mathbf{s}), Y(\mathbf{s})|\widehat{\boldsymbol{\delta}}\right)$. Here $\widehat{\boldsymbol{\delta}}$ is the oridinary least squares (OLS) estimator and $\mathcal{T}_1(\mathbf{h}(p,q))$ and $\mathcal{T}_2(\mathbf{h}(p,q))$ are prespecified tolerance regions with centroid of $\mathbf{h}(p,q)$. Then the weighted-least squares (WLS) method (see Cressie (1993), pp.96) based on the empirical semivariogram in (29) is employed to obtain the estimates of the covariance parameters which minimize the weighted sum of squares error (WSSE) defined as

$$W(\boldsymbol{\Theta}) \equiv \sum_{p=-P}^{P} \sum_{q=-Q}^{Q} \sum_{u=0}^{U} |N(\mathbf{h}(p,q); u)| \left\{\frac{\widehat{\gamma}(\mathbf{h}(p,q); u)}{\gamma(\mathbf{h}(p,q); u|\boldsymbol{\Theta})} - 1\right\}^2, \tag{31}$$

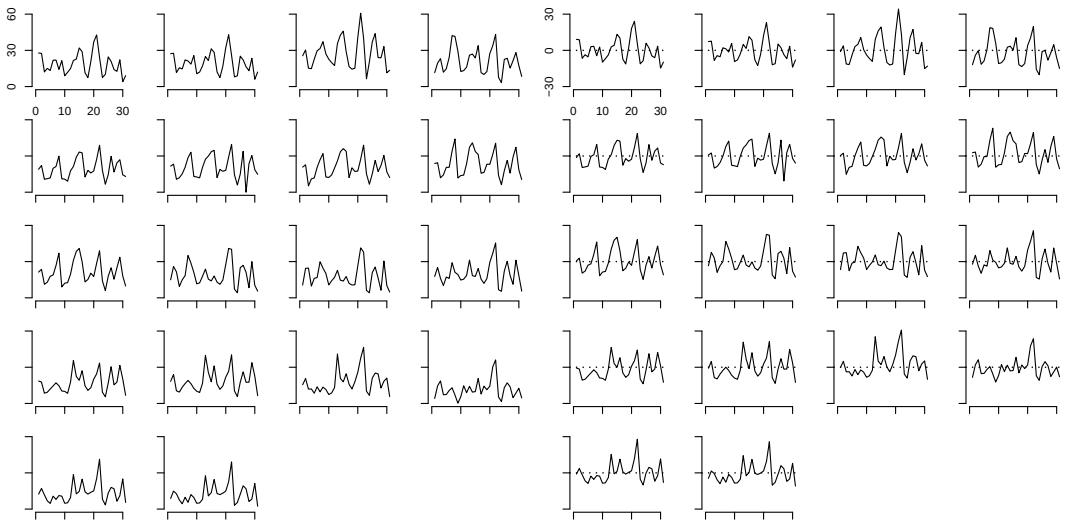

(a) $Z(\mathbf{s}, t)$ (b) $\widetilde{Z}(\mathbf{s}, t)$

Figure 7: Time-series plots of the original measuremnts, $Z(\mathbf{s}, t)$ and the residuals, $\widetilde{Z}(\mathbf{s}, t)$ for the 18 monitoring stations; the measuring unit for $PM_{2.5}$ is $\mu g/m^3$.

where $\gamma(\mathbf{h}(p, q); u|\boldsymbol{\Theta})$ is the theoretical spatial-temporal semivariogram with parameters $\boldsymbol{\Theta}$. We also consider the maximum likelihood (ML) estimation method for obtaining the covariance parameter estimates. In order to simplify the construction of asymmetric covariance models, the spatial trend, $g(X(\mathbf{s}_i), Y(\mathbf{s}_i)|\boldsymbol{\delta})$ is removed from the original measurments by considering second-order polynomial function with geodesic distances transformed from the position information (longitudes and latitudes) prior to the estimation of the covariance parameters $\boldsymbol{\Theta}$ by the two methods. Figure 7 shows the time-series plots of the original $PM_{2.5}$ concentrations and the residuals for the 18 monitoring stations. From Figure 7(b), one can see that, since the spatial pattern looks quite similar and each time-series does not seem to have certain violations against weak stationarity, the spatial-temporal process of the detrended $PM_{2.5}$ concentrations satisfies stationarity in space as well as in time.

Now we explain the result from the analysis of $PM_{2.5}$ daily concentration dataset. The parameter

Table 1: Parameter Estimation based on Exponential Asymmetric Spatial-Temporal Covariance from WLS and ML methods.

$\boldsymbol{\Theta}$	**M.1**		**M.2**		**M.3**		**M.4**	
	WLS	ML	WLS	ML	WLS	ML	WLS	ML
σ	3.5365	2.4738	3.6281	2.4190	3.5356	2.5240	3.6286	2.4134
ϕ	118.73	87.600	117.20	93.045	118.38	86.469	117.15	119.03
α	0.0011	0.0016	0.0008	0.0010	0.0011	0.0015	0.0008	0.0019
β	0.8556	0.8766	0.9004	1.0000	0.6459	0.3357	0.9000	0.5085
v_{11}			0.0006	0.0010			0.0006	0.0003
v_{12}			–.0010	–.0015			–.0010	–.0010
v_{21}					–236.0	894.14	–.3873	858.37
v_{22}					–493.2	121.46	–.6891	140.63
WSSE	936.44		882.30		928.63		882.30	
$-\log(L)$		1590.82		1580.44		1585.78		1576.60

estimation methods are performed with the spatially detrended $PM_{2.5}$ concentrations, $\left\{\widetilde{Z}(\mathbf{s},t)\right\}$. For the WLS estimation, we set $\mathcal{T}_1(\mathbf{h}(p,q)) = \mathcal{T}_2(\mathbf{h}(p,q)) = 25$, $P = 5$, $Q = 3$, and $U = 4$ in (30) and (31). So, for example, $\mathbf{h}(-P,-Q) = (-250,-150)$ and $\mathbf{h}(0,Q) = (0,150)$. The WSSE in (31) and the negative log-likelihood ($-\log(L)$) are minimized using the routine `nlminb` in `R`. Table 1 shows the estimates of $\boldsymbol{\Theta}$ from the WLS and the ML methods for each model (**M.1**–**M.4**). In terms of **M.1** and **M.2**, the estimates are quite similar regardless of the estimation method except that the WLS estimate of partial sill (ϕ) is larger than the ML one. However, in case of **M.3**, there is a big difference of partial sill between the estimation methods, and, moreover, the asymmetry vector, $\mathbf{v}_2$ has different sign. Unlike the first three models (**M.1**–**M.3**), **M.4** based on the ML method has much larger partial sill, which is almost same as the corresponding WLS estimate. One possible interpretation can be that the partial sill is overestimated by the ML method in order to compensate for the increase of the denominator, $1 - \mathbf{v}_1'\mathbf{v}_2$ in **M.4** whereas the WLS estimates of

asymmetry vectors ($\mathbf{v}_1$, $\mathbf{v}_2$) does not influence any change of the partial sill, that is, $1 - \mathbf{v}_1'\mathbf{v}_2 \approx 1$. Now we compare symmetric or asymmetric spatial-temporal coavariance models by means of the objective functions, WSSE and $-\log(L)$. Table 1 displays the criteria helpful to find out which model is best for this dataset. In terms of the objective functions, any asymmetric covariance model performs better than the symmetric one.

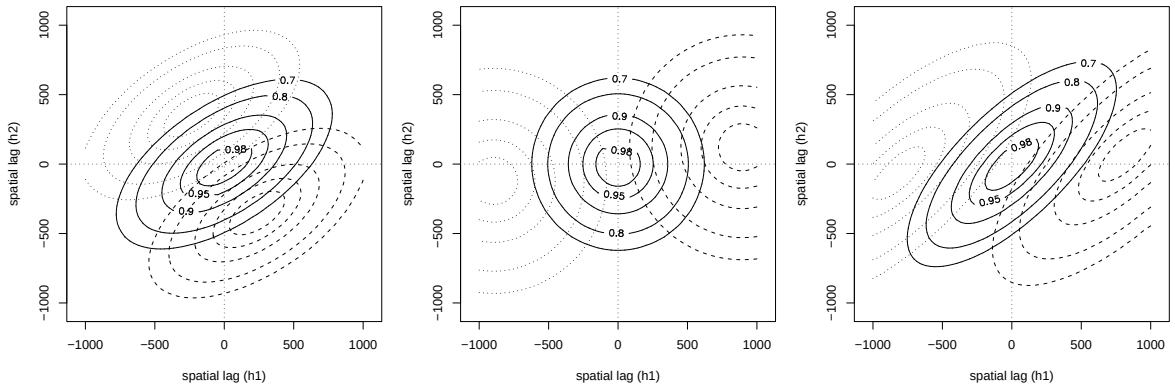

(a) **M.2** (b) **M.3** (c) **M.4**

Figure 8: The Contour Plots of asymmetric covariance models (**M.2**–**M.4**) based on the ML estimates shown in Table 1. Note that dotted line is for $u = -1$, solid line for $u = 0$, and dashed line for $u = 1$.

What is important here is that we can implicitly determine the movements of the asymmetric covariance models, **M.2** through **M.4** by taking a look at Figure 8. As you can see, the asymmetric covariances roughly move from west to east as the time lag, u increases. This implies that the correlation between arbitrary two locations changes as u changes, and, therefore, the asymmetry parameter vector makes the neigborhood structure for each location different.

Based on the ML estimates for each model (see Table 1), we predict the $PM_{2.5}$ concentrations at the preassigned grids on the three consecutive dates, August 25, 2003 through August 27, 2003. Figure 9 shows that **M.1** through **M.3** produce very similar kriging maps and **M.4** has much

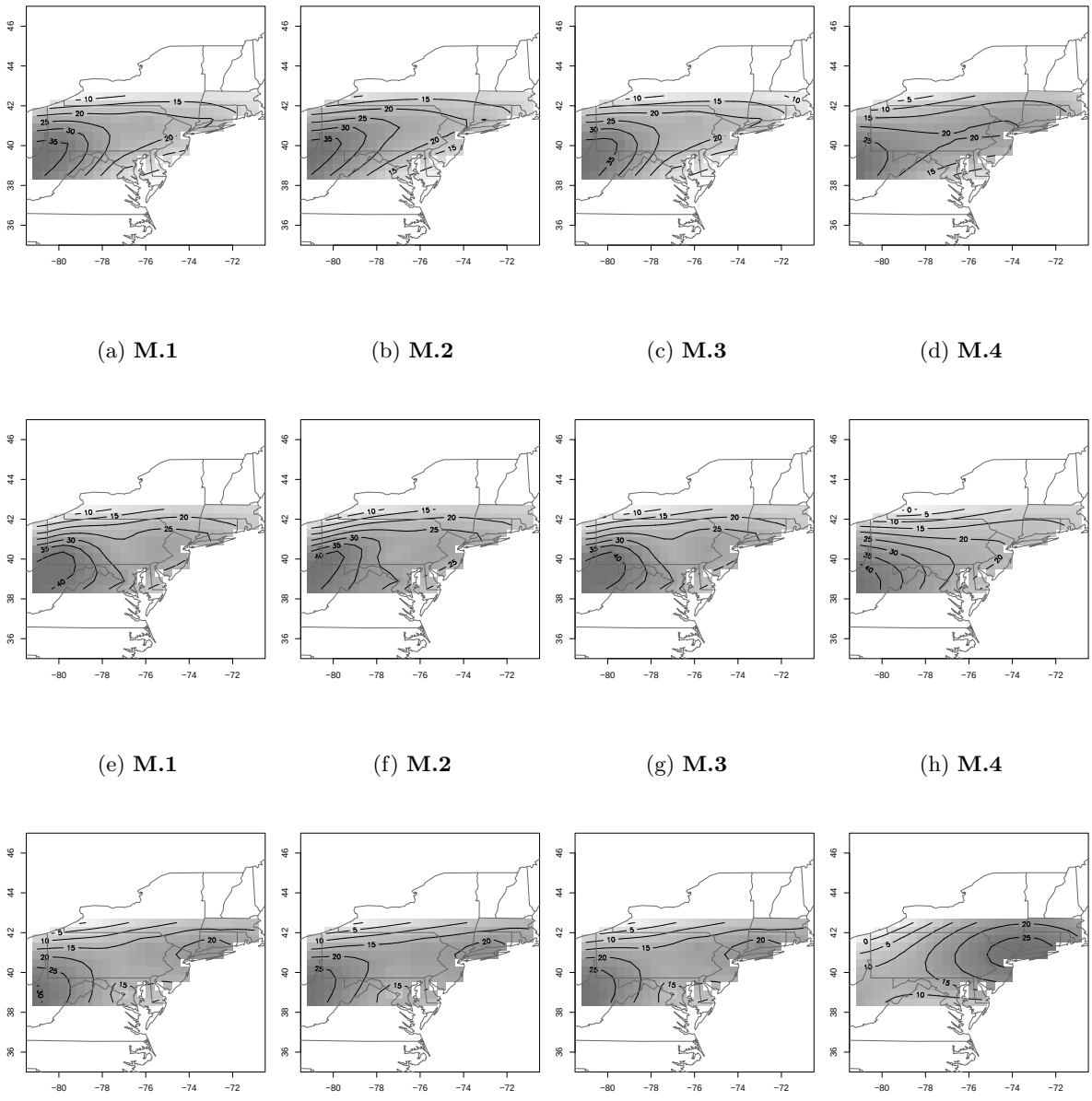

(a) **M.1** (b) **M.2** (c) **M.3** (d) **M.4**

(e) **M.1** (f) **M.2** (g) **M.3** (h) **M.4**

(i) **M.1** (j) **M.2** (k) **M.3** (l) **M.4**

Figure 9: Kriging maps based on the ML estimates in Table 1. Note that the prediction (spatial interpolation) is performed at the regular grids on the three consecutive dates; August 25, 2003 (top row), August 26, 2003 (second row), and August 27, 2003 (bottom row).

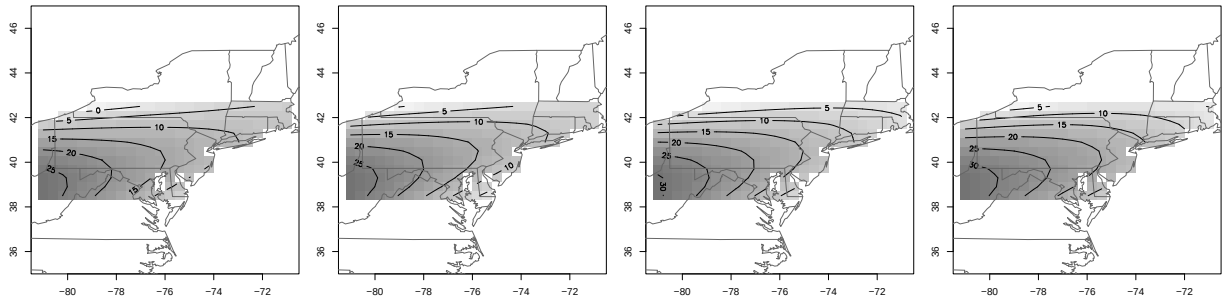

(a) **M.1** (b) **M.2** (c) **M.3** (d) **M.4**

Figure 10: Kriging maps based on the ML estimates in Table 1 on September 1, 2003.

smoother spatial pattern than the others. It is also possible to forecast $PM_{2.5}$ concentrations in the near future, for example, at $(T+1)$ time although main goal of the spatial-temporal covariance models proposed in this study is the prediction inside the given space-time domain (Figure 10).

In this section, we have applied a new class of asymmtric spatial-temporal covariance models to the $PM_{2.5}$ daily concentrations at the FRM monitoring stations in the northeastern U.S. From the data analysis, we found out that the spatial-temporal processes based on asymmetric covariance functions explain the given dataset better than the process based on simple covariance function in terms of the objective functions.

6 Discussion

In this study, we introduced new concepts of symmetry in spatial-temporal processes and proposed classes of asymmetric stationary spatial-temporal covariance models. Since these covariances are just Fourier transformations of the corresponding valid spectral density functions, they can easily be shown to be positive definite. Unlike a process with separable, even nonseparable covariance, an asymmetric spatial-temporal process is influenced by spatial-temporal dependencies, which are mainly controled by asymmetry parameters. This characteristic is very helpful to analyze the air-

pollution data affected by some external metheological conditions, for instance, wind speed, wind direction, air pressure and so on.

The asymmetric covariance models can be extended to the spatial domain with $d > 2$ although our results presented in this study are based on the two-dimensional spatial domain. Posssible expressions of a spectral density function yielding a nonstationary symmetric covariance function can be as follow:

$$f_{\Delta_j}(\boldsymbol{\omega};\tau) = \gamma_j \left(\alpha_j^2\beta_j^2 + \beta_j^2\|\boldsymbol{\omega} + \tau\mathbf{v}_1\|^2 + \alpha_j^2(\tau + \mathbf{v}_2'\boldsymbol{\omega})^2\right)^{-\nu_j},$$

or

$$f_{\Delta_j}(\boldsymbol{\omega};\tau) = \gamma_j \left(\alpha_j^2 + \|\boldsymbol{\omega} + \tau\mathbf{v}_1\|^2\right)^{-\nu_j} \left(\beta_j^2 + (\tau + \mathbf{v}_2'\boldsymbol{\omega})^2\right)^{-\nu_j},$$

where $j = 1, \cdots, k$ is the index of subregion satisfying stationarity, and Δ_j is the center of the j-th subregion. As one part of our further work, we are estimating the parameters by means of Bayesian approach taking into account uncertainties in the covariance models.

Appendix

Suppose that the $(d+1)$ dimensional spectal density function is defined as

$$f_0(\boldsymbol{\omega};\tau) \equiv \gamma(\alpha^2\beta^2 + \beta^2\|\boldsymbol{\omega}\|^2 + \alpha^2\tau^2)^{-\nu},$$

γ, α and β are positive, and $\nu > \frac{d+1}{2}$. Then the corresponding covariance function can be derived like the following way:

$$\begin{aligned} C_0(\mathbf{h};u) &= \int_{\mathbb{R}}\int_{\mathbb{R}^d} f_0(\boldsymbol{\omega};\tau)\exp\{i\mathbf{h}'\boldsymbol{\omega} + iu\tau\}d\boldsymbol{\omega}\, d\tau \\ &= \gamma\int_{\mathbb{R}}\exp\{iu\tau\}\int_{\mathbb{R}^d}\left\{\alpha^2\left(\beta^2+\tau^2\right) + \beta^2\|\boldsymbol{\omega}\|^2\right\}^{-\nu}\exp\{i\mathbf{h}'\boldsymbol{\omega}\}d\boldsymbol{\omega}\, d\tau. \end{aligned}$$

By Stein (2005),

$$\begin{aligned}
&\int_{\mathbb{R}^d} \left\{\alpha^2\left(\beta^2+\tau^2\right)+\beta^2\|\boldsymbol{\omega}\|^2\right\}^{-\nu} \exp\{i\mathbf{h}'\boldsymbol{\omega}\}d\boldsymbol{\omega} \\
&= \frac{\pi^{d/2}\beta^{-2\nu}}{2^{\nu-d/2-1}\Gamma(\nu)}\left\{\frac{\alpha}{\beta}\sqrt{\beta^2+\tau^2}\right\}^{-2\nu+d}\mathcal{M}_{\nu-d/2}\left(\frac{\alpha}{\beta}\sqrt{\beta^2+\tau^2}\|\mathbf{h}\|\right),
\end{aligned}$$

where $\mathcal{M}_\nu(r) = r^\nu \mathcal{K}_\nu(r)$. And, by Gradshteyn and Ryzhik (2000, pp.730, Eq.6.726 4),

$$\begin{aligned}
\mathcal{L}_\nu(\mathbf{h};u) &\equiv \int_{\mathbb{R}} \left(\beta^2+\tau^2\right)^{-(\nu-d/2)/2}\mathcal{K}_{\nu-d/2}\left(\frac{\alpha}{\beta}\sqrt{\beta^2+\tau^2}\|\mathbf{h}\|\right)\exp\{iu\tau\}d\tau \\
&= 2\int_0^\infty \left(\beta^2+\tau^2\right)^{-(\nu-d/2)/2}\mathcal{K}_{\nu-d/2}\left(\frac{\alpha}{\beta}\sqrt{\beta^2+\tau^2}\|\mathbf{h}\|\right)\cos\{u\tau\}d\tau \\
&= \sqrt{2\pi}(\alpha\|\mathbf{h}\|)^{-\nu+d/2}\beta^{-\nu+d/2+1}\mathcal{M}_{\nu-\frac{d+1}{2}}\left(\beta\sqrt{\frac{\alpha^2}{\beta^2}\|\mathbf{h}\|^2+u^2}\right).
\end{aligned}$$

Then we can obtain the closed form of the $(d+1)$ dimensional covariance function given by

$$\begin{aligned}
C_0(\mathbf{h};u) &= \frac{\gamma\pi^{d/2}\|\mathbf{h}\|^{\nu-d/2}}{2^{\nu-d/2-1}\Gamma(\nu)}\alpha^{-\nu+d/2}\beta^{-\nu-d/2}\mathcal{L}_\nu(\mathbf{h};u) \\
&= \frac{\gamma\pi^{(d+1)/2}\alpha^{-2\nu+d}\beta^{-2\nu+1}}{2^{\nu-(d+1)/2-1}\Gamma(\nu)}\mathcal{M}_{\nu-\frac{d+1}{2}}\left(\beta\sqrt{\frac{\alpha^2}{\beta^2}\|\mathbf{h}\|^2+u^2}\right).
\end{aligned}$$

References

[1] Cressie, N., 1993. Statistics for spatial data. John Wiley & Sons.

[2] Cressie, N., Huang, H.-C., 1999. Classes of nonseparable, spatio-temporal stationary covariance functions. J. Amer. Statist. Assoc. 94, 1330–1340.

[3] Fuentes, M., Chen, L., Davis, J., Lackmann, G., 2005. Modeling and predicting complex space-time structures and patterns of coastal wind fields. Environmetrics 16, 449–464.

[4] Gneiting, T., 2002. Nonseparable, stationary covariance functions for space-time data. J. Amer. Statist. Assoc. 97, 590–600.

[5] Golam Kibria, B. M., Sun, L., Zidek, J. V., Le, N. D., 2002. Bayesian spatial prediction of random space-time fields with application to mapping $PM_{2.5}$ exposure. J. Amer. Statist. Assoc. 97, 112–124.

[6] Gradshteyn, I. S., Ryzhik, I. M., 2000. Table of Integrals, Series, and Products, sixth Ed. Academic Press.

[7] Jones, R. H., Zhang, Y., 1997 Models for continuous stationary space-time processes. in Modelling Longitudinal and Spatially Correlated Data, Lecture Notes in Statistics 122, (eds.) T. G. Grogorie, D. R. Brillinger, P. J. Diggle, E. Russek-Cohen, W. G. Warren, and R. D. Wolfinger, pp. 289–298. Springer.

[8] Jun, M., Stein, M. L., 2004. An approach to producing space-time covariance functions on spheres. Technical Report 18, CISES, the University of Chicago.

[9] Lu, N., Zimmerman, D. L., 2005. Testing for directional symmetry in spatial dependence using the periodogram. J. Statist. Plan. Inference. 129, 369–385.

[10] Myers, D. E., Journel, A. G., 1990. Variograms with zonal anisotropies and noninvertible kriging systems. Mathematical Geology 22, 779–785.

[11] Rodriguez-Iturbe, I., Mejia, J. M., 1974. The design of rainfall newtorks in time and space. Water Resources Research 10, 713–729.

[12] Rouhani, S., Hall, T. J., 1989. Space-time kriging of groundwater data. (ed.) M. Amstrong, Geostatistics, v. 2, pp. 639–651. Kluwer Academic Publisher.

[13] Rouhani, S., Myers, D. E., 1990. Problems in space-time kriging of geohydrological data. Mathematical Geology 22, 611–623.

[14] Scaccia, L., Martin, R. J., 2005. Testing axial symmetry in separability in lattice processes. J. Statist. Plan. Inference 131, 19–39.

[15] Stein, M. L., 2005. Space-time covariance functions. J. Amer. Statist. Assoc. 100, 310–321.

[16] Zidek, J. V., 1997. Interpolating air pollution for health impact assessment. In Statistics for Environment 3: Pollution Assessment and Control, (eds.) V. Barnett, and K. Feridun Turkman, New York, Wiley, pp. 251-268.